FINAL TECHNICAL REPORT

U.S. Geological Survey
National Earthquake Hazard Reduction Program
Award No. G12AP20056

Award Title

Paleoseismic investigation of an active fault scarp subparallel to the main trace of the San Andreas Fault at the Bidart Fan Site in the Carrizo Plain

Principal Investigators and Report Authors:

Lisa Grant Ludwig
Sinan O. Akciz

Contact Address:

Program in Public Health
653 E. Peltason Dr., AIRB 2085
University of California, Irvine
Irvine, CA 92697-3957
Phone: (949)824-2889 or 824-5491; fax: (949) 824-0529
Email: lgrant@uci.edu

Start date: 04/15/2012
End date: 04/14/2014

ABSTRACT

The San Andreas Fault (SAF) is the most significant source of seismic hazard in Southern California. Recent field reconnaissance, ground penetrating radar (GPR) investigations, and LiDAR image analysis suggested that a previously recognized linear structural anomaly sub-parallel to the main trace of the SAF between Wallace Creek and the Bidart Fan is a fault that cuts late Holocene sedimentary deposits of the Bidart Fan. We excavated two paleoseismic trenches across the anomaly to confirm prior surface rupture and investigate recency and style of deformation. Trenches revealed distinct stratigraphy which included fissures, upward termination of faults, vertical apparent offset, lateral unit thickness changes, and colluvial wedges, exposing evidence for at least five, and possibly six, surface rupturing earthquakes. Preliminary results of analysis of 18 detrital charcoal samples indicate that these five earthquakes occurred since ~2,900 B.C. The two youngest ruptures occurred within the last 1650 years (since ~360 A.D.) Compared to the paleoseismic record at the Bidart Fan site, which is approximately 400 m to the SW, almost all of the Bidart Fault earthquakes (with the exception of MRE) are much older. Thus, the Bidart fault does not appear to rupture as often as the main strand of the SAF, despite its proximity to it. We suspect the youngest rupture occurred during the 1857 Fort Tejon earthquake, but we can't confirm it through radiocarbon or other dating methods. We speculate that the Bidart Fault strand ruptures during the largest magnitude earthquakes along the southern SAF, but this hypothesis is not testable with existing data. Similarly, we cannot confirm that deposition across the Bidart strand fault has been sufficient to record all ruptures during the past 4900 years, or if this record is representative of earthquakes on this strand. If the record of Bidart Fault ruptures reported herein is complete, the recurrence intervals are an order of magnitude longer than the main strand of the SAF (< 100 yrs vs. 1000 yrs). We speculate that 1857 surface slip between Wallace Creek and Bidart Fan could have been ~7 m (5.5±1.5 m) distributed over the main trace of the SAF and the Bidart Fault strands.

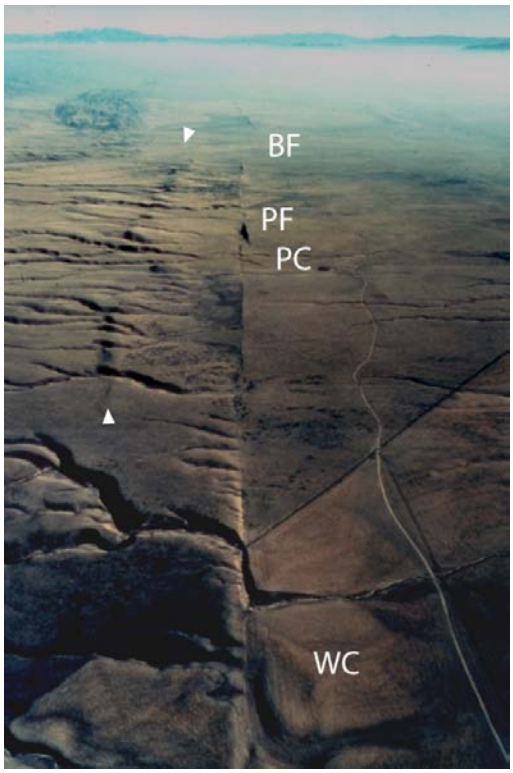

INTRODUCTION

Figure 1. Aerial photograph of the linear main trace of the San Andreas fault in the Carrizo Plain, and the geomorphic structural anomaly located sub-parallel to it (in between white triangles). View is looking southeast. Important slip rate study sites are Wallace Creek (WC) and Phelan Creeks (PC). Important paleoseismic study sites are Phelan Fan (PF) and Bidart Fan (BF).

Purpose and scope

An important objective of the USGS Earthquake Hazards Reduction Program is to estimate the probabilities of future large-magnitude earthquakes on known active faults, using the best available science and data (Field, 2007; Field et al. 2009). These data include spatial and temporal distribution of surface rupturing earthquakes along the faults in question, and their magnitudes. The San Andreas fault (SAF) is the most significant source of seismic hazard in California and its proximity to densely populated and economically vital regions makes the risk associated with this fault a major threat to the nation as well as the state. In this project, we examine the surface rupture history of a subsidiary strand of the SAF, herein named the "Bidart Fault", that was only recently recognized.

Background

Surface slip reconstructions of past earthquakes serve to formulate conceptual models for the recurrence of earthquakes along faults. One of the most influential reconstructions was made for the 1857 earthquake (Sieh, 1978) and preceding earthquakes (Sieh and Jahns, 1984) along

the surface rupture trace of the south-central SAF. It became a cornerstone in the formulation of the characteristic earthquake (Schwartz and Coppersmith, 1984) and uniform slip models which are now widely applied in seismic hazard analysis and earthquake forecasts (e.g. Field et al., 2009).

The results of 3-D excavation studies along the main strand of the SAF in the Carrizo Plain (Figure 1) yield different measurements of slip from the 1857 earthquake between Wallace Creek (~5.5-8 m slip measured by Liu et al., 2004; Liu-Zeng et al., 2006) and Phelan Fan (6.7 m slip measured by Grant and Sieh, 1993). Results of excavation studies also differ considerably from measurements of slip derived by analysis of topographic data along a ~60 km section of the SAF in the Carrizo Plain (~5.5 m reported by Zielke et al., 2010). It not clear if the different slip measurements reflect along-strike slip variation during the 1857 Fort Tejon earthquake, as proposed by Grant and Sieh, (1993), or differing number of slip events at different study sites, as proposed by Grant Ludwig et al. (2010). Another possible explanation, which we explore in this study, is that previously undocumented structures accommodated additional slip during each rupture of the SAF main trace, or by additional "off cycle" earthquakes between main SAF ruptures.

Geomorphology of the Bidart Scarp

In the area between Wallace Creek and Bidart Fan, a structural anomaly sub-parallel to the main trace of the SAF is observed and has been recognized for decades as a geomorphic feature of Late to Latest Quaternary age. As shown in Figure 1 (between white triangles) it has positive geomorphic expression on the northeast side of the main SAF trace. It is subparallel to the main trace, with prominent expression between Wallace Creek and an unnamed alluvial fan adjacent to the northwest margin of the Bidart Fan of Grant and Sieh (1994).

This structure has been interpreted as a broad antiform over a blind fault (K. Sieh, personal communication, 1989-1993). The antiformal section of the structure is shown on Figure 2A, mapped in orange. This structure has never been seriously considered to have been active during the past several earthquakes, because it appeared to die out and be buried by Holocene alluvial fan deposits. However, during analysis of the B4 LiDAR data set (Bevis et al., 2005) and field reconnaissance efforts, we recognized that the southeastern continuation of this structure does deform the latest Holocene deposits of the Bidart Fan, as shown in Figure 2(B) and Figure 3.

Prior GPR investigation:

With funding from the Southern California Earthquake Center (SCEC) we conducted a ground penetrating radar (GPR) survey of the proposed excavation site in 2010. Like many other locations we have surveyed in the Carrizo Plain, subsurface GPR data does not show a clear structure which can be interpreted as a fault. However, we identified a positive anomaly which coincides with a surface channel along the scarp near Elkhorn Road (Figure 3). The anomaly (Figure 4) terminates abruptly at the scarp, and coincides with a subtle ~2 m right-lateral jog in the surface channel.

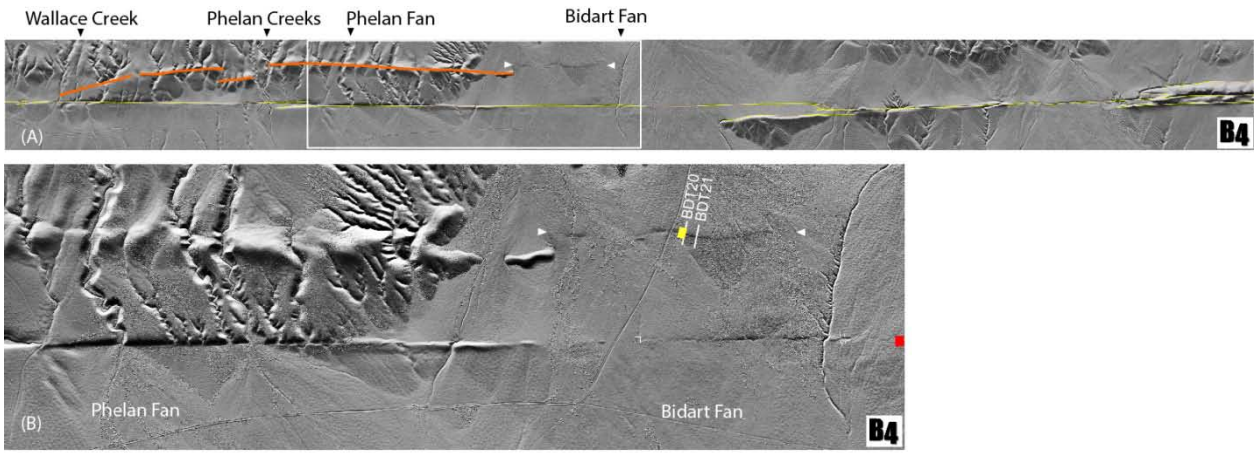

Figure 2. (A) Shaded relief image of a section of the SAF in the Carrizo Plain based on B4 Lidar data. Shaded relief map downloaded from http://www.Opentopography.org. Yellow lines are the fault traces. Orange line is the structural anomaly subparallel to the SAF whose relation to the main trace of the SAF is unknown. White triangles are located at the end points of a linear scarp which clearly deforms the late Holocene deposits at the Bidart Fan. (B). Close-up view of the boxed area in Figure 2(A) with the locations of trenches BDT20 and BDT21 marked with white lines. Red box shows the area excavated between 2005 and 2009which provided ages of the last six earthquakes on the main trace of the SAF at the Bidart Fan site (Akciz et al., 2010). Yellow box shows the area surveyed with a ground penetrating radar (GPR), as shown in Figure 4.

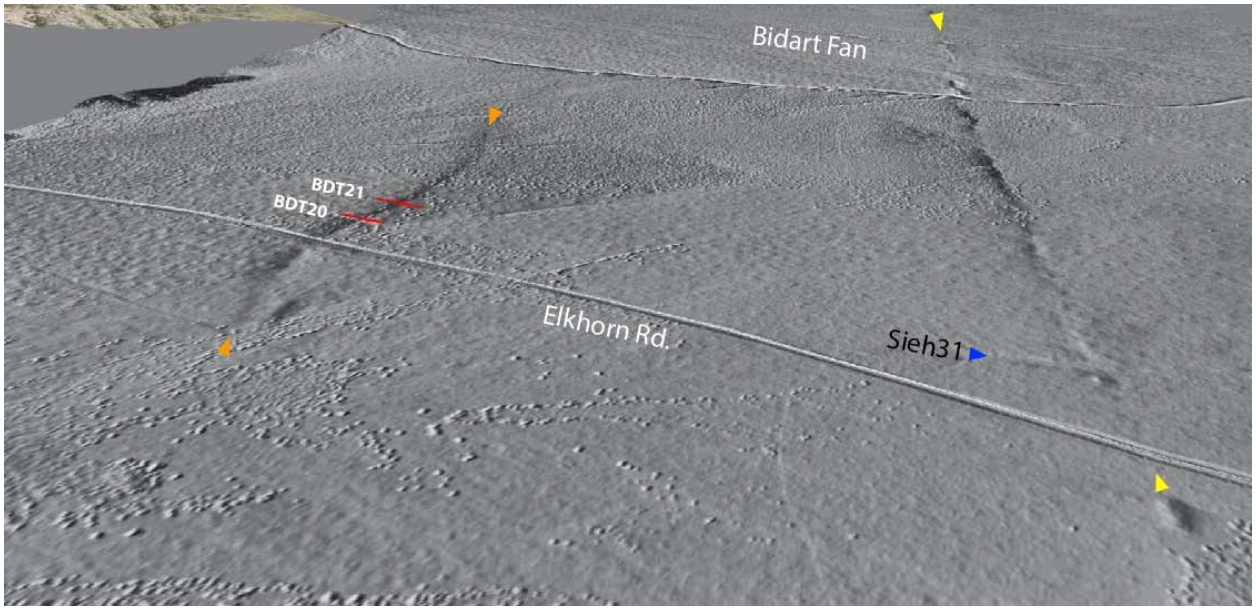

Figure 3 Oblique view of B4 LiDAR (Bevis et al., 2005) shaded relief map of the study site, looking southeast. Orange triangles indicate the location of the newly recognized "Bidart Fault scarp". Trenches BDT20 and BDT21 (red lines) were excavated in 2012. Trench sites were selected where the scarp morphology is well defined. A small channel crosses the scarp between Elkhorn Rd. and BDT20. Yellow triangles show the location of the main trace of the SAF. The main trace scarp was enhanced during the 1857 Fort Tejon earthquake. Morphological similarities suggest that Bidart Fault scarp was recently rejuvenated, possibly during the 1857 rupture of the main trace. Blue triangle labeled "Sieh 31" shows the location of offset channel #31 of Sieh (1978), which is currently being investigated by Akciz et al. (2014) and Kleber et al. (2014).

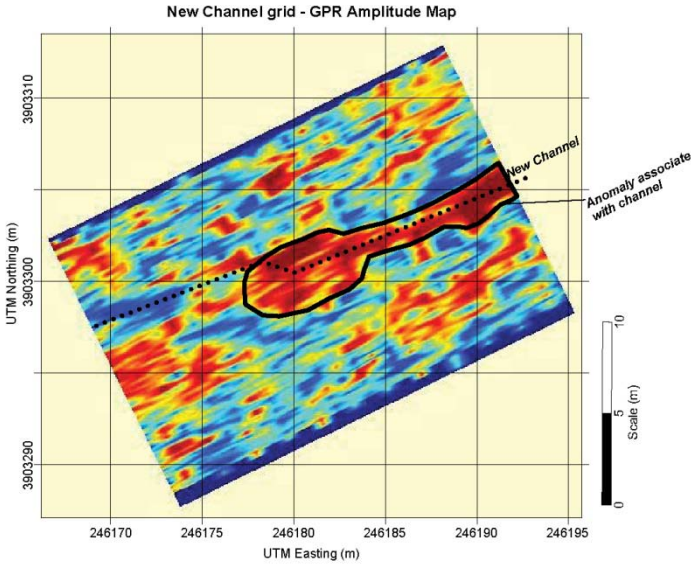

Figure 4. GPR data depth slice at 0.2 m below the surface collected at the proposed excavation site. Dotted line is the trace of the thalweg of the channel recorded with a Trimble XH GPS unit with a tornado antenna. Boundary of the positive anomaly which coincided with the upstream end of the surveyed channel (dashed line) is also marked.

RESEARCH ACTIVITIES

In 2012, we excavated two paleoseismic trenches, BDT20 and BDT21, "trenches 20 and 21", across the Bidart Fault scarp to investigate prior surface rupture, and recency and style of deformation. The trenches revealed distinct alluvial fan stratigraphy with prominent expressions of faulting, including fissures, upward termination of faults, vertical apparent offset, lateral unit thickness changes, and colluvial wedges. In the Appendix, we present logs of the southeast walls of both trenches.

Evidence of surface ruptures

Multiple surface ruptures, with clear expression, were observed in both walls of both trenches. In the Appendix, logs of the southeastwalls of both trenches have been annotated with letters (circled) at the locations of surface rupture evidence. An excerpt of the trench log from the southeast wall of BDT21 is shown in Figure 5. Clear cross-cutting relationships exposed on the walls of trench BDT21 indicated evidence for five surface rupturing earthquakes, labelled A through E. At the time of writing of this report, we are analyzing data and evidence for a possible 6th earthquake, located between events C and D. Since that analysis has not been completed, our dating efforts, and the following discussion in this report, focus on the presence, ages, and significance of 5 surface ruptures.

Dates of ruptures

We collected samples of organic materials, which were sparsely disseminated throughout the alluvial sediments. The samples included in-situ burned grass fragments, charred twigs, and unidentified detrital charcoal pieces. The samples were analyzed at the Keck Carbon Cycle AMS facility at UC Irvine.

Results of radiocarbon dating are displayed in Table 1A and Table 1B. With one exception, all sample dates are middle to late Holocene age. We used Oxcal (Ramsay, 2007) to constrain the dates of ruptures A through E. Figure 6 shows results of preliminary analysis of all 18 detrital samples, and approximate ages of the last 5 surface ruptures, as constrained by the pdf ages of the samples. All five events, A through E, occurred in the late Holocene, since 2,900 B.C, as shown on Figure 6.

Based on radiocarbon ages, the two youngest ruptures occurred within the last 1,650 years. Assuming that no major surface rupture has occurred since 1857, the results of Oxcal analysis indicate that Events A and B occurred within the time period 361 A.D. to 1857 A.D.

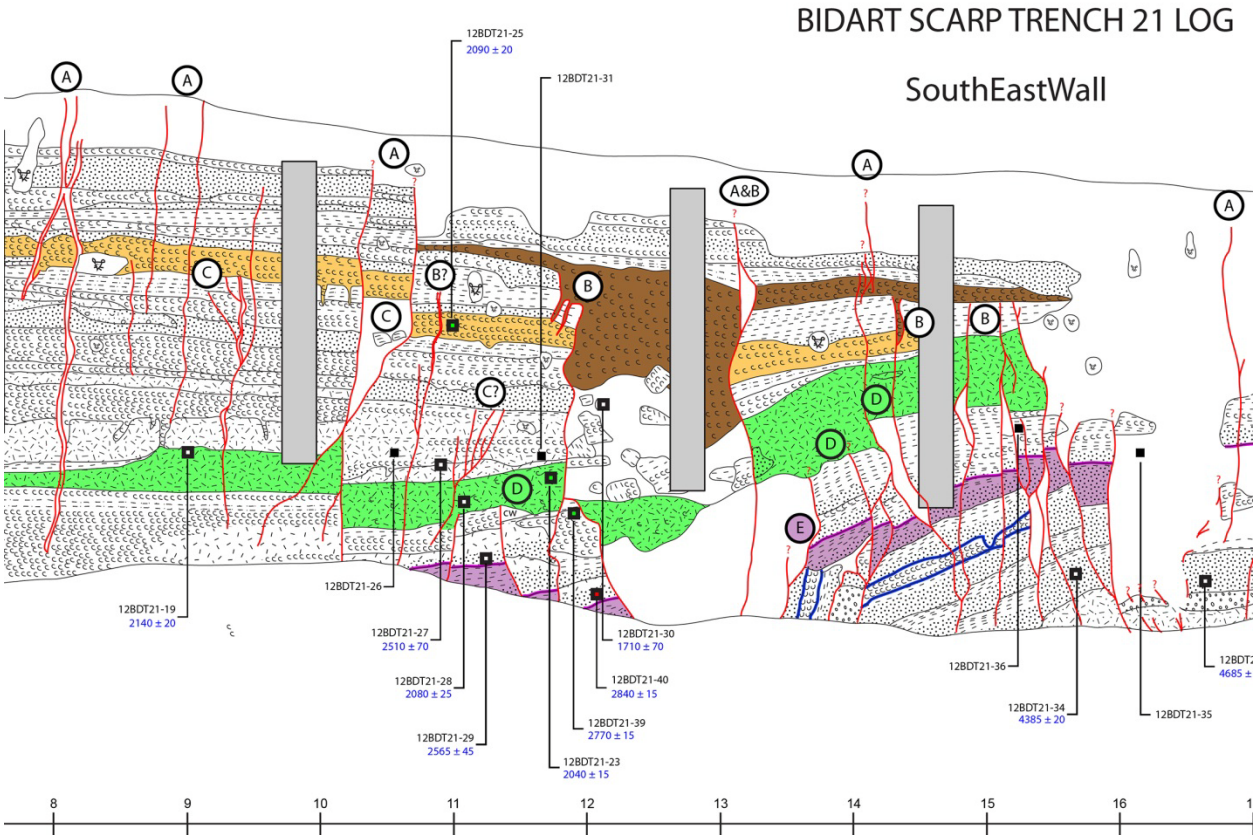

Figure 5. An excerpt from the log of the southeast wall of trench BDT21, looking to the southeast. Tic marks along the horizontal line at the bottom are at 1 meter intervals. Prominent units are colored to show style of deformation. The clay-rich brown unit fills in a large fissure. The green silt unit displays ~2 m of apparent vertical deformation. Organic sample locations are marked with squares. Black squares represent samples that have been collected from the southeast wall, but not dated. Open boxes with white fill represent dated samples from the southeast wall. Red and green filled boxes are samples from the northwest wall, with locations projected onto this log. Green filled samples are dated. Each sample number is labelled in black type. The radiocarbon ages (BP) are labelled in blue. Refer to Table 1A for Radiocarbon lab data. Red sub-vertical lines indicate mapped faults. The location of each rupture event horizon is marked with capital letter A,B,C,D and E. Some evidence suggests the presence of a 6th event, between events D and C.

TABLE 1A - RADIOCARBON DATING RESULTS FROM TRENCH BDT21

KECK CARBON CYCLE AMS FACILITY
EARTH SYSTEM SCIENCE DEPT, UC IRVINE

^{14}C results Akciz/Grant-Ludwig Aug 09 2012

UCIAMS #	Sample name	Other ID	$d^{13}C$ (‰)	±	fraction Modern	±	$D^{14}C$ (‰)	±	^{14}C age (BP)	±
112750	12BDT21-1 .11mgC				0.7994	0.0017	-200.6	1.7	1800	20
112751	12BDT21-3 .017mgC				0.0238	0.0192	-976.2	19.2	>22300	
112752	12BDT21-7 .015mgC				0.7793	0.0086	-220.7	8.6	2000	90
112753	12BDT21-8				0.7971	0.0014	-202.9	1.4	1820	15
112754	12BDT21-16 .013mgC				0.7937	0.0100	-206.3	10.0	1860	110
112755	12BDT21-19				0.7661	0.0016	-233.9	1.6	2140	20
112756	12BDT21-21				0.7647	0.0014	-235.3	1.4	2155	20
112757	12BDT21-23				0.7759	0.0014	-224.1	1.4	2040	15
112758	12BDT21-25 .14mgC				0.7710	0.0016	-229.0	1.6	2090	20
112759	12BDT21-27 .025mgC				0.7320	0.0055	-268.0	5.5	2510	70
112760	12BDT21-28 .069mgC				0.7720	0.0024	-228.0	2.4	2080	25
112761	12BDT21-29 .042mgC				0.7268	0.0038	-273.2	3.8	2565	45
112762	12BDT21-30 .021mgC				0.8084	0.0061	-191.6	6.1	1710	70
112763	12BDT21-32 .044mgC				0.5727	0.0040	-427.3	4.0	4480	60
112764	12BDT21-33 .15mgC				0.5582	0.0016	-441.8	1.6	4685	25
112765	12BDT21-34				0.5793	0.0011	-420.7	1.1	4385	20
112766	12BDT21-39				0.7082	0.0013	-291.8	1.3	2770	15
112767	12BDT21-40				0.7023	0.0012	-297.7	1.2	2840	15

Radiocarbon concentrations are given as fractions of the Modern standard, $D^{14}C$, and conventional radiocarbon age, following the conventions of Stuiver and Polach (Radiocarbon, v. 19, p.355, 1977).

Sample preparation backgrounds have been subtracted, based on measurements of ^{14}C-free wood.

All results have been corrected for isotopic fractionation according to the conventions of Stuiver and Polach (1977), with d13C values measured on prepared graphite using the AMS spectrometer. These can differ from □^{13}C of the original material, if fractionation ocurred during sample graphitization or the AMS measurement, and are not shown.

Comments:
A large fraction of the submitted samples dissolved during pretreatment or were too small to measure.
The large uncertainties for some of these results are due to the very small sample sizes.
The 14C/C ratio for sample 12BDT21-3 was within two standard deviations of zero after background subtraction and the corresponding radiocarbon age is quoted as a 2 sigma lower limit.

TABLE 1B – RADIOCARBON DATING RESULTS FROM TRENCH BDT20

KECK CARBON CYCLE AMS FACILITY
EARTH SYSTEM SCIENCE DEPT, UC IRVINE

^{14}C results Akciz Mar 12 2013

UCIAMS #	Sample name	Other ID	$d^{13}C$ (‰)	±	fraction Modern	±	$D^{14}C$ (‰)	±	^{14}C age (BP)	±
122081	12BDT20-3				0.7644	0.0011	-235.6	1.1	2160	15
122082	12BDT20-5 .015mgC				0.6421	0.0124	-357.9	12.4	3560	160
122083	12BDT20-6				0.7635	0.0012	-236.5	1.2	2165	15
122084	12BDT20-10				0.7647	0.0011	-235.3	1.1	2155	15
122085	12BDT20-15 .021mgC				0.7677	0.0082	-232.3	8.2	2120	90
122086	12BDT20-17 .058mgC				0.7191	0.0034	-280.9	3.4	2650	40
122087	12BDT20-18 .015mgC				0.7871	0.0117	-212.9	11.7	1920	120
122088	12BDT20-22				0.8180	0.0012	-182.0	1.2	1615	15
122089	12BDT20-23				0.8108	0.0012	-189.2	1.2	1685	15

Radiocarbon concentrations are given as fractions of the Modern standard, $D^{14}C$, and conventional radiocarbon age, following the conventions of Stuiver and Polach (Radiocarbon, v. 19, p.355, 1977).

Sample preparation backgrounds have been subtracted, based on measurements of ^{14}C-free wood.

All results have been corrected for isotopic fractionation according to the conventions of Stuiver and Polach (1977), with d13C values measured on prepared graphite using the AMS spectrometer. These can differ from $\delta^{13}C$ of the original material, if fractionation ocurred during sample graphitization or the AMS measurement, and are not shown.

Comments:
The large uncertainties for some of these samples are due to the small sample sizes.
Sample 12BDT 20-13 was too small and could not be measured.

Evidence for the most recent surface rupturing earthquake includes several cm-scale fissures, and surface terminating fault traces with apparent lateral separations. We know that the main trace of the SAF ruptured in 1857, with ~ 5m slip at the nearby Bidart Fan (Grant Ludwig et al., 2010; Zielke et al., 2010). Based on the geomorphic expression of the scarp, and near-surface traces, we suspect that Event A on the Bidart Fault is the 1857 Fort Tejon earthquake. However, there is no conclusive evidence to support this interpretation.

We compare the dates of Bidart Fault surface ruptures with dates of SAF main trace ruptures reported by Akciz et al. (2010) and Grant Ludwig et al. (2010) at the Bidart Fan paleoseismic site, approximately 400 m to the SW. For comparison, the Oxcal age plot for surface ruptures A through E reported by Akciz et al. (2010) is excerpted in Figure 7.

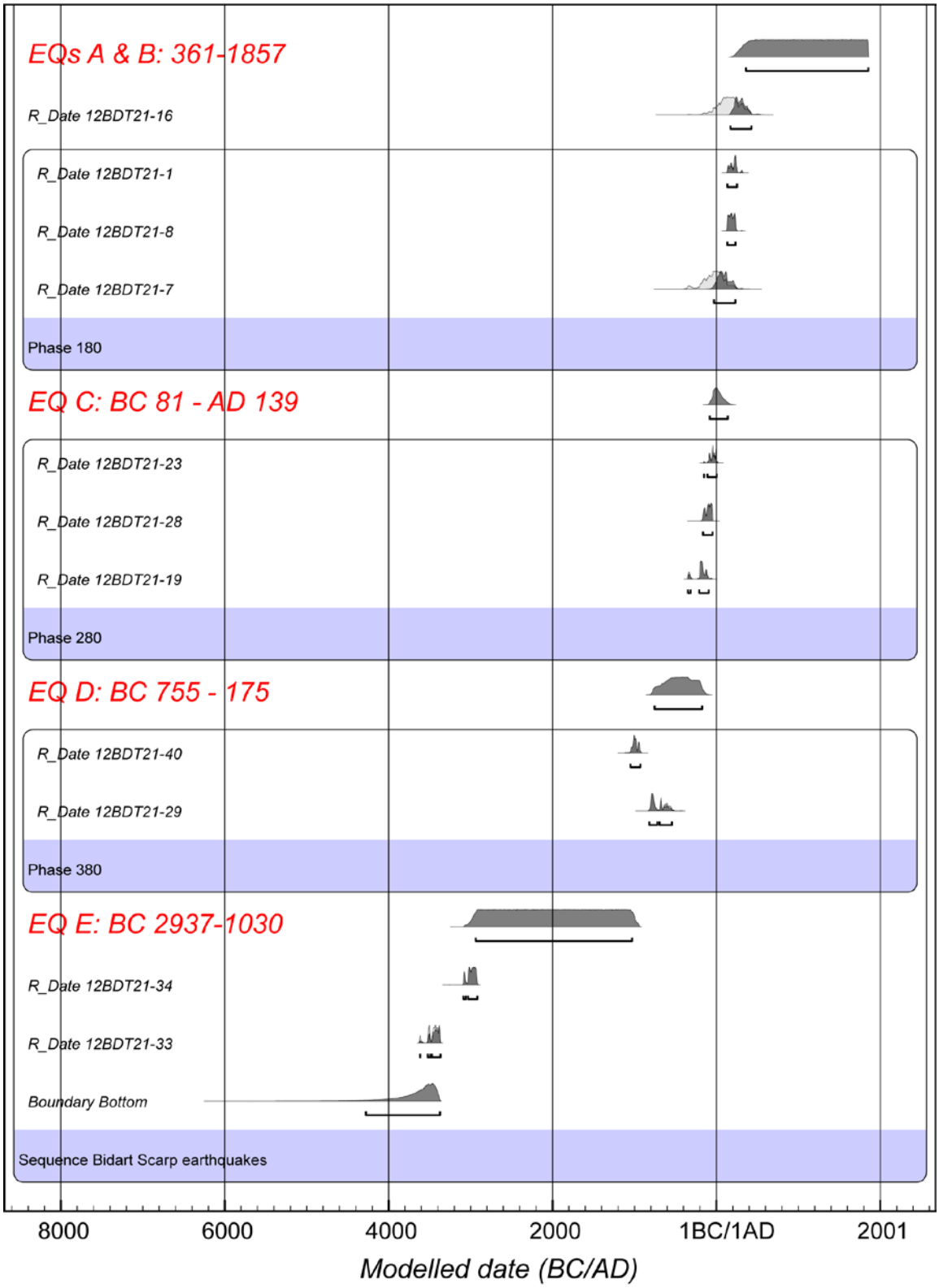

Figure 6 – Oxcal plot (Ramsay, 2007) showing radiocarbon age pdfs of dated samples, and resulting constraints on ages of Bidart Fault surface rupturing earthquakes A through E.

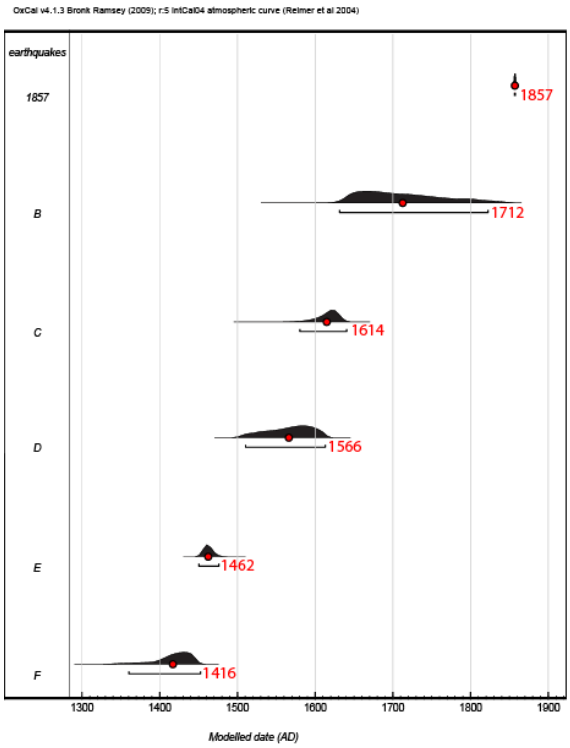

Figure 7 – Dates of surface ruptures A through E at the Bidart Fan paleoseismic site on the main trace of the SAF (from Akciz et al., 2010).

With the exception of the most recent event, which is poorly constrained to occur between 361 and 1857 A.D., all of the Bidart Fault earthquakes are older than ruptures of the main strand. If the record of Bidart Fault ruptures observed in trenches 20 and 21 is complete, then the recurrence intervals are an order of magnitude longer than the main strand of the San Andreas (< 100 yrs vs. ~1000 yrs).

Surface slip

If the most recent event (MRE), event A, on the Bidart Fault is indeed the 1857 earthquake, then slip on the Bidart fault might explain some of the spatial slip variation or discrepancies reported by other studies. Figure 8 shows a small channel which if right-laterally offset approximately 1.5 m across the Bidart Fault scarp. The two youngest Bidart Fault ruptures, A and B, occurred within the last 1650 yrs. This channel could have been offset by Event A, or Event B, or both.

Figure 8. ~1.5 m right-laterally offset channel near the SE termination of the exposed section of the Bidart fault. Red lines mark the locations of the proposed trench locations. White box indicates the approximate extend of the 3D excavation.

Summary

Preliminary results from two trenches indicate that the Bidart Fault, a strand of the SAF in the Carrizo Plain, has ruptured 5 or 6 times since 2,900 B.C. The two youngest ruptures occurred within the last 1,650 years with the most recent earthquake (MRE) likely occurring during the 1857 Fort Tejon earthquake. Compared to the paleoseismic record at the Bidart Fan site, which is approximately 400 m to the SW, almost all of the Bidart Fault earthquakes (with the exception of MRE) are much older. Thus, the Bidart fault does not appear to rupture as often as the main strand of the SAF, despite its proximity to it. If the record of Bidart Fault ruptures reported herein is complete, the recurrence intervals are an order of magnitude longer than the main strand of the SAF (< 100 yrs vs. ~1000 yrs). We speculate that 1857 surface slip between Wallace Creek and Bidart Fan could have been ~7 m (5.5±1.5 m) distributed over the main trace of the SAF and the Bidart Fault strands.

REFERENCES

Akciz, S.O., Grant Ludwig, L., Arrowsmith, J R., Zielke, O., 2010. Century-long average time intervals between earthquake ruptures of the San Andreas fault in the Carrizo Plain, California: Geology, v. 38, p. 787-790.

Akciz, S. O., Grant Ludwig, L., Zielke*, O., and Arrowsmith, J R., Post-1857 fracturing and deflection of an apparent offset channel along the San Andreas fault in the Carrizo Plain. *Bull. Seismol. Soc. Amer.,* Accepted July 14, 2014.

Akciz, S. O., Grant Ludwig[+], L**.,** Halford, D., Marliyani, G. I., Salisbury, J. B., Kleber, E. J., Arrowsmith, J, R., Rhodes, E. and Capaldi, T. (2014). Multi-method measurement of offset from the 1857 Fort Tejon earthquake along the San Andreas fault in the Carrizo Plain at channel Seih31, *Seismological Research Letters*, v. 85, no. 2, p. 518.

Bevis, M., et al., (2005), The B4 Project: Scanning the San Andreas and San Jacinto fault zones, EOS Trans. AGU, 86(52), Fall Meet. Suppl., Abstract H34B-01.

Field, E. H. (2007). Review Article: A summary of previous Working Groups on California Earthquake Probabilities, Bull. Seismol. Soc. Amer., 97, no. 4, 1033-1053, doi: 10.1785/0120060048.

Field, E. H., Dawson, T. E., Felzer, K. R., Frankel, A. D., Gupta, V., Jordan, T. H., Parsons, T., Petersen, M. D., Stein, R. S., Weldon II, R. J., and Wills C. J., (2009). Uniform California Earthquake Rupture Forecast, Version 2 (UCERF2), Bull. Seismol. Soc. Am. 99, no. 4, 2053-2107, doi: 10.1785/0120080049.

Grant, L.B., and Sieh, K., 1993. Stratigraphic Evidence for 7 Meters of Dextral Slip on the San-Andreas-Fault During the 1857 Earthquake in the Carrizo Plain: Bulletin of the Seismological Society of America, v. 83, p. 619-635.

Grant, L. B. and K. Sieh, Paleoseismic Evidence of Clustered Earthquakes on the San Andreas Fault in the Carrizo Plain, California, *Journal of Geophysical Research*, v. 99, no. B4, p.6819-6841, 1994.

Grant Ludwig, L., Akciz, S.O**.,** Noriega, G. R., Zielka, O., Arrowsmith, J R., 2010**.** Climate-Modulated Channel Incision and Rupture History of the San Andreas Fault in the Carrizo Plain: Science, 327, 5969, p. 1117-1119.

Kleber, E. J., Arrowsmith, J R., Akciz, S. O., Salisbury, J. B., Grant Ludwig, L**.**, Halford, D., Delong, S. B., Marliyani, G. I., Henderson, W. M., (2014). 3D investigation of channel morphology across the San Andreas fault zone using structure from motion and terrestrial laser scanning. *Seismological Research Letters*, v. 85, no. 2, pg. 545

Liu, J., Klinger, Y., Sieh, K., and Rubin, C., 2004. Six similar sequential ruptures of the San Andreas fault, Carrizo Plain, California: Geology, v. 32, p. 649-652.

Liu-Zeng, J., Y. Klinger, K. Sieh, C. Rubin, and G. Seitz, 2006. Serial ruptures of the San Andreas fault, Carrizo Plain, California, revealed by three-dimensional excavations: *J. Geophys. Res.*, 111, B02306, doi:10.1029/2004JB003601.

Schwartz, D.P., and K. Coppersmith, Fault behavior and characteristic earthquakes – examples from the Wasatch and San Andreas fault zones, J. Geophys. Res, 89, 5681-5689, 1984.

Ramsey, C.B. (2007). OxCal Program, v. 4.0, Radiocarbon Accelerator Unit, University of Oxford, UK; https://c14.arch. ox.ac.uk/oxcal.html

Sieh, K. E., 1978. Slip along the San Andreas fault associated with the great 1857 earthquake, *Bull. Seis. Soc. Am*., *68(5),* 1421-1448.

Sieh, K.E., Jahns, R.H., 1984. Holocene activity of the San Andreas fault at Wallace Creek, California. Geological Society of America Bulletin 95, 883–896.

Zielke, O., Arrowsmith, J R., Ludwig L G., Akciz, S.O.**,** 2010**.** Slip in the 1857 and Earlier Large Earthquakes Along the Carrizo Plain, San Andreas Fault**:** Science, 327, 5969, p. 1119-1122.

BIBLIOGRAPHY OF ALL PUBLICATIONS RESULTING FROM THIS AWARD

Grant Ludwig, L., and Akciz, S. O. (2014) Paleoseismic investigation of an active fault scarp subparallel to the main trace of the San Andreas Fault at the Bidart Fan Site in the Carrizo Plain, Final Technical Report, National Earthquake Hazard Reduction Program Award No. G12AP20056 (This report).

Grant Ludwig, L**.**, Akciz, S. O., Cheiffetz, T. and Sato, T. (2013). Discovery and paleoseismic investigation of the Bidart fault, a subparallel oblique-slip strand of the San Andreas fault in the Carrizo Plain. *Seismological Research Letters*, v. 84, no 2, March/April 2013, p. 332.

Cheiffetz, T. M., Sato, T., Akciz, S. and Grant Ludwig, L**.** (2012). Discovery and paleoseismic investigation of the Bidart Fault, a subparallel oblique-slip strand of the San Andreas fault in the Carrizo Plain, *Southern California Earthquake Center 2012 Annual Meeting Program*, abstract p.95 , poster # 252, Sept 8-12, 2012.

BIDART SCARP TRENCH 21 LOG

SouthEastWall

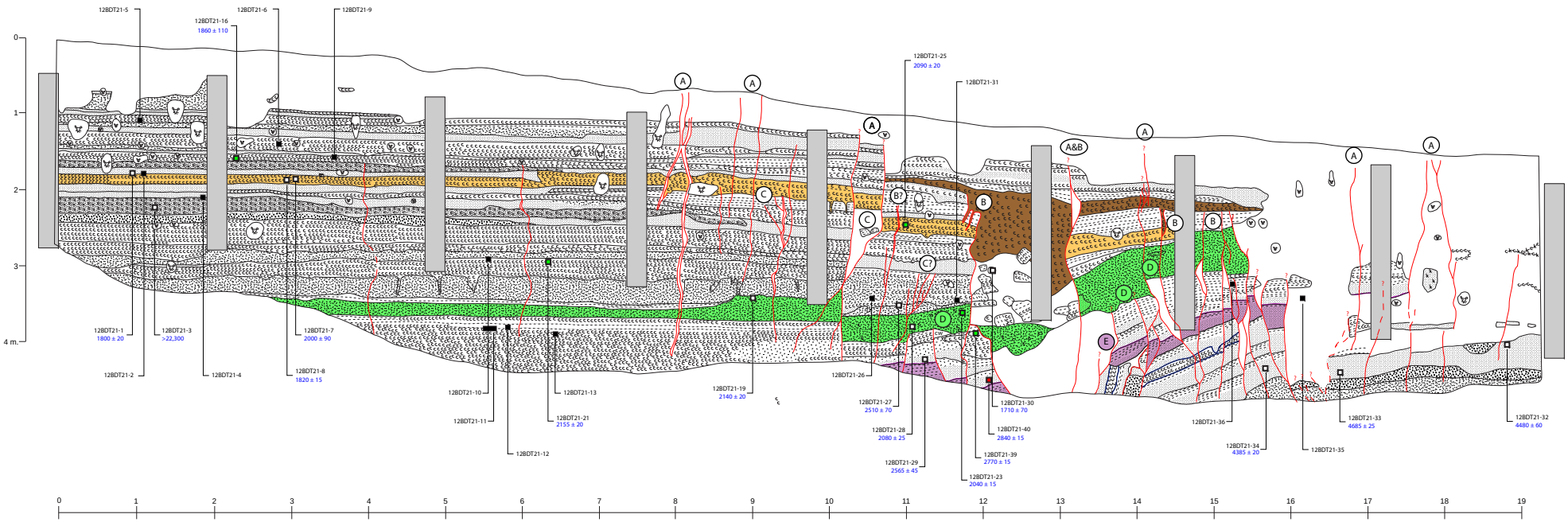

BIDART SCARP TRENCH 20 LOG
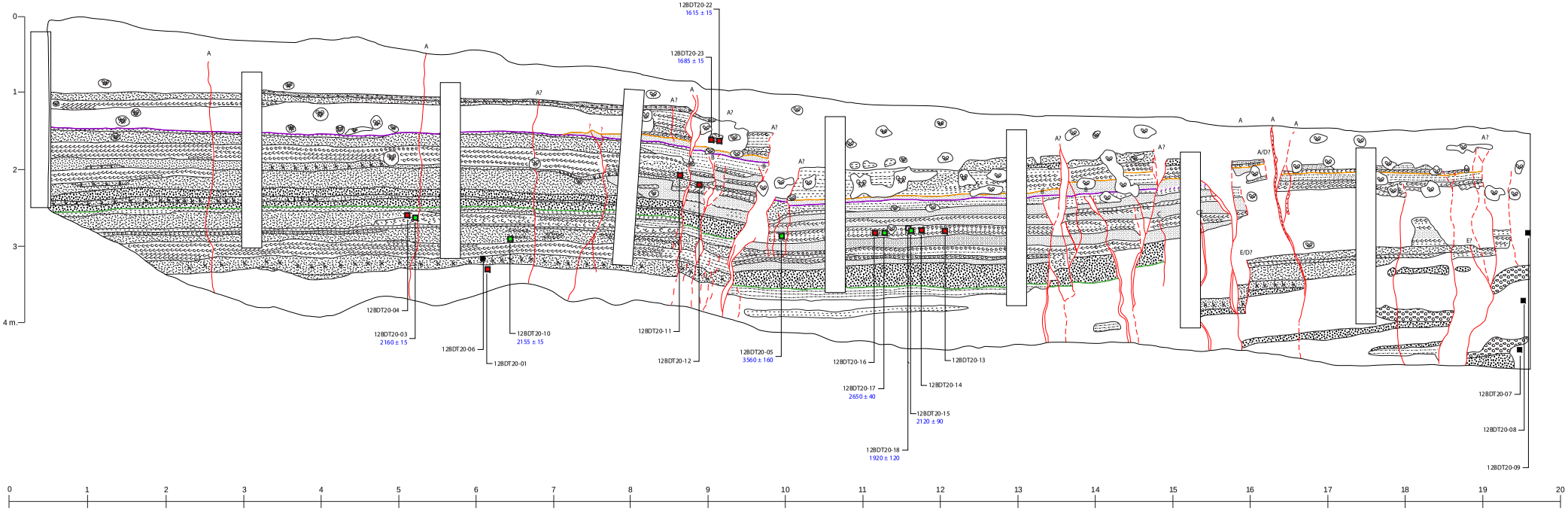
SouthEastWall